ORIGINAL ARTICLE

Internal doses in experimental mice and rats following exposure to neutron-activated $^{56}MnO_2$ powder: results of an international, multicenter study

Valeriy Stepanenko[1] · Andrey Kaprin[2] · Sergey Ivanov[1] · Peter Shegay[2] · Kassym Zhumadilov[3] · Aleksey Petukhov[1] · Timofey Kolyzhenkov[1] · Viktoria Bogacheva[1] · Elena Zharova[2] · Elena Iaskova[1] · Nailya Chaizhunusova[4] · Dariya Shabdarbayeva[4] · Gaukhar Amantayeva[4] · Arailym Baurzhan[4] · Bakhyt Ruslanova[4] · Zhaslan Abishev[4] · Madina Apbassova[4] · Ynkar Kairkhanova[4] · Darkhan Uzbekov[4] · Zaituna Khismetova[4] · Yersin Zhunussov[4] · Nariaki Fujimoto[5] · Hitoshi Sato[6] · Kazuko Shichijo[7] · Masahiro Nakashima[7] · Aya Sakaguchi[8] · Shin Toyoda[9] · Noriyuki Kawano[10] · Megu Ohtaki[5] · Keiko Otani[10] · Satoru Endo[11] · Masayoshi Yamamoto[12] · Masaharu Hoshi[10]

Abstract

The experiment was performed in support of a Japanese initiative to investigate the biological effects of irradiation from residual neutron-activated radioactivity that resulted from the A-bombing. Radionuclide ^{56}Mn ($T_{1/2} = 2.58$ h) is one of the main neutron-activated emitters during the first hours after neutron activation of soil dust particles. In our previous studies (2016–2017) related to irradiation of male Wistar rats after dispersion of $^{56}MnO_2$ powder, the internal doses in rats were found to be very inhomogeneous: distribution of doses among different organs ranged from 1.3 Gy in small intestine to less than 0.0015 Gy in some of the other organs. Internal doses in the lungs ranged from 0.03 to 0.1 Gy. The essential pathological changes were found in lung tissue of rats despite a low level of irradiation. In the present study, the dosimetry investigations were extended: internal doses in experimental mice and rats were estimated for various activity levels of dispersed neutron-activated $^{56}MnO_2$ powder. The following findings were noted: (a) internal radiation doses in mice were several times higher in comparison with rats under similar conditions of exposure to $^{56}MnO_2$ powder. (b) When 2.74×10^8 Bq of $^{56}MnO_2$ powder was dispersed over mice, doses of internal irradiation ranged from 0.81 to 4.5 Gy in the gastrointestinal tract (small intestine, stomach, large intestine), from 0.096 to 0.14 Gy in lungs, and doses in skin and eyes ranged from 0.29 to 0.42 Gy and from 0.12 to 0.16 Gy, respectively. Internal radiation doses in other organs of mice were much lower. (c) Internal radiation doses were significantly lower in organs of rats with the same activity of exposure to $^{56}MnO_2$ powder (2.74×10^8 Bq): 0.09, 0.17, 0.29, and 0.025 Gy in stomach, small intestine, large intestine, and lungs, respectively. (d) Doses of internal irradiation in organs of rats and mice were two to four times higher when they were exposed to 8.0×10^8 Bq of ^{56}Mn (in comparison with exposure to 2.74×10^8 Bq of ^{56}Mn). (e) Internal radiation doses in organs of mice were 7–14 times lower with the lowest $^{56}MnO_2$ amount (8.0×10^7 Bq) in comparison with the highest amount, 8.0×10^8 Bq, of dispersed $^{56}MnO_2$ powder. The data obtained will be used for interpretation of biological effects in experimental mice and rats that result from dispersion of various levels of neutron-activated $^{56}MnO_2$ powder, which is the subject of separate studies.

Keywords ^{56}Mn · Neutron activation · Dispersion of radioactivity · Radioactive dust · Internal irradiation · Experimental mice and rats

Introduction

Our experiments were performed in support of a Japanese initiative to investigate the biological effects of irradiation from residual neutron-activated radioactivity that resulted from the A-bombing (Hoshi 2020). During nuclear

✉ Valeriy Stepanenko
mrrc@mrrc.obninsk.ru

Extended author information available on the last page of the article

explosions that take place in the atmosphere, neutron-activated radionuclides are distributed in surface layers of the soil, contributing to the beta and gamma irradiation that results from residual radioactivity. The main radionuclides are ^{24}Na, ^{28}Al, ^{31}Si, ^{32}P, ^{38}Cl, ^{42}K, ^{45}Ca, ^{46}Sc, ^{56}Mn, ^{59}Fe, ^{60}Co, and ^{134}Cs (Weitz 2014). Radionuclide ^{56}Mn ($T_{1/2} = 2.58$ h) is one of the main neutron-activated emitters during the first hours after neutron activation of soil dust particles (Tanaka et al. 2008; Weitz 2014). The purpose of this international multicenter study was to extend our previous work (Shichijo et al. 2017; Stepanenko et al. 2017) to estimate internal doses for laboratory animals (mice and rats) with different exposures to ^{56}MnO$_2$ in the form of dispersed powder. The results of the internal dose assessments will be used to investigate the biological effects that result from this type of exposure, which will be the subject of future publications.

Materials and methods

Table 1 gives details of the laboratory mice and rats used in the experiments and also the initial ^{56}Mn activity (100 mg ^{56}MnO$_2$ powder sprayed over the animals while they were in their cages).

The total numbers of mice and rats targeted for dosimetry only were 24 and 9, respectively. Along with the animals scheduled for dosimetry, animals that were intended for subsequent biological studies were additionally placed in the same cages. As a result, the total number of animals in each cage for each irradiation was different, from 6 to 9 rats and from 3 to 10 mice per cage.

All experimental work was performed during 2018–2019 at research reactor IVG.1 ("Baikal-1") located in the territory of the Semipatinsk nuclear test site (Lanin 2013), Republic of Kazakhstan. Details of neutron activation of MnO$_2$ powder (Rare Metallic Co., Ltd) and exposure of animals to dispersed ^{56}MnO$_2$ particles were presented in our previous paper (Stepanenko et al. 2017). Briefly, experimental animals were placed in special boxes for exposure to ^{56}MnO$_2$ powder (Fig. 1). One hundred milligrams of activated powder was used for each ^{56}MnO$_2$ exposure. Statistical distribution of MnO$_2$ particle sizes is presented in Fig. 2. Animals were exposed
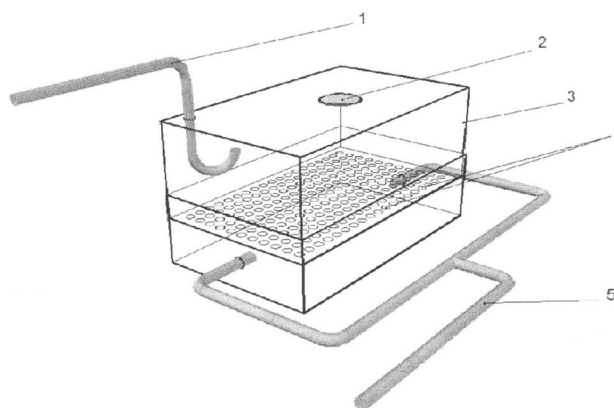
Fig. 1 Schematic view of the box where neutron-activated radioactive ^{56}MnO$_2$ powder was dispersed on experimental animals. 1-Pneumatic tube for dispersion of radioactive ^{52}Mn powder; 2-air filter; 3-plastic wall of the box; 4-plastic floor of the box with holes, where experimental animals were placed; 5-tubes for forced ventilation

Table 1 Laboratory mice and rats (supplier: Kazakh Scientific Center of Quarantine and Zoonotic Diseases, Almaty, Kazakhstan under contract with Charles River Laboratories, Germany) and initial activity of neutron-activated ^{56}MnO$_2$ powder used for spraying over animals in each cage)

Date of exposure	Laboratory animals	Initial ^{56}Mn activity in 100 mg ^{56}MnO$_2$ powder used for spraying over the animals in each cage**)
17.08.2018	CD-1 mice, 11-week-old male	2.74×10^8 Bq
17.08.2018	Wistar rats, 11-week-old male	2.74×10^8 Bq
18.08.2018	Wistar rats, 11-week-old male	5.5×10^8 Bq
18.08.2018	Wistar rats, 11-week-old male	8.0×10^8 Bq
22.04.2019	C57BL mice, 10-week-old male	8.0×10^8 Bq
22.04.2019	C57BL mice, 10-week-old male	2.74×10^8 Bq
23.04.2019	C57BL mice, 10-week-old male	8.0×10^7 Bq
17.06.2019	C57BL mice, 10-week-old male	2.74×10^8 Bq
17.06.2019	BALB/C mice, 10-week-old male	2.74×10^8 Bq
18.06.2019	C57BL mice, 10-week-old male	8.0×10^8 Bq
18.06.2019	BALB/C mice, 10-week-old male	8.0×10^8 Bq

As a result of irradiation of 100 mg MnO$_2$ by thermal neutrons with fluence $F = 1.2 \times 10^{14}$ neutron/cm^2, the yield of ^{56}Mn activity (Ao) is equal to 8×10^7 Bq. The ratio Ao/F is equal to 6.7×10^{-7} Bq per thermal neutron/cm^2

**Numbers of animals in each cage for each irradiation were different—from 6 to 9 (rats) and from 3 to 10 (mice) animals per cage

Fig. 2 Statistical distribution of MnO$_2$ particle diameters. Vertical axis: frequency, relative units. Horizontal axis- diameter of particles, μm. Mean diameter of MnO$_2$ particles is equal to 8.1 μm
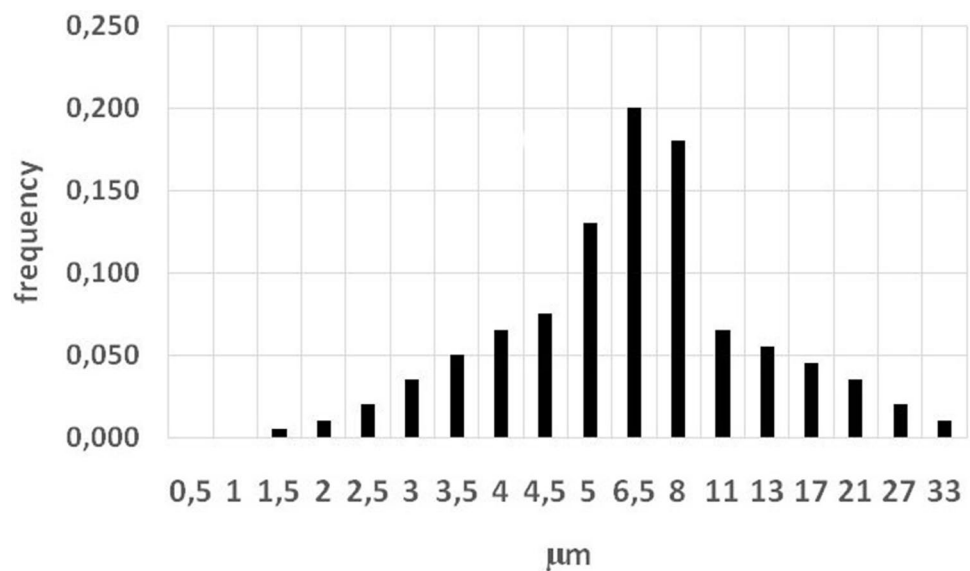

for 1 h. Exposed animals were removed from cages and euthanized by injection of an excessive dose of pentobarbital. All work with experimental animals was approved by the ethics committee of Semey State Medical University, Kazakhstan, according to directive 2010/63/EU of the European Parliament and the Council of the Office on protection of animals used for scientific purposes of 22 September 2010 (Directive 2010/63/EU 2010). The following organs and tissues were surgically extracted from experimental animals: lungs, heart, small intestine, large intestine, stomach, esophagus, liver, spleen, kidney, trachea, skin, eyes, and blood. To measure specific activity of ^{56}Mn, small pieces (about 1 ml) of each organ were weighed and subjected to gamma-spectrometry by an AMPTEC, Inc., Gamma-Rad5 spectrometer with an NaI(Tl) detector. Details of measurement conditions and calibration of the spectrometer were presented in our previous paper (Stepanenko et al. 2017). A description of internal dose estimations according to the Medical Internal Radiation Dose methodology (Bolch et al. 2009) was presented in the same paper. According to MIRD methodology, internal radiation doses were assessed by taking into account accumulated activity of ^{56}Mn in all studied organs (which are listed above), self-irradiation of these

organs, and their irradiation by all other sampled organs and tissues. Calculation of absorbed fractions of energy in studied organs from beta and gamma irradiation of ^{56}Mn was performed using the Monte-Carlo method (Briemeister 2000) and age-dependent mathematical phantoms of rats and mice (Stepanenko et al. 2015). The spectrum of ^{56}Mn beta particles (Stabin et al. 2001) was accounted for internal dose calculations. Gamma irradiation from ^{56}Mn (Be et al. 2013) was accounted for as well.

Results

Each extracted sample of organs (lungs, heart, small intestine, large intestine, stomach, esophagus, liver, spleen, kidney, trachea, skin, eyes, and blood) from all investigated laboratory animals was subjected to gamma spectrometry in a well-shielded room. Volumes of extracted samples were small enough (about 1 ml) to consider them as radiating point sources in comparison with distance to and size of the spectrometer's detector. The highest ^{56}Mn specific activities were found in large and small intestine, stomach, lungs, and skin, which corresponds to our previous results obtained from similar experiments on
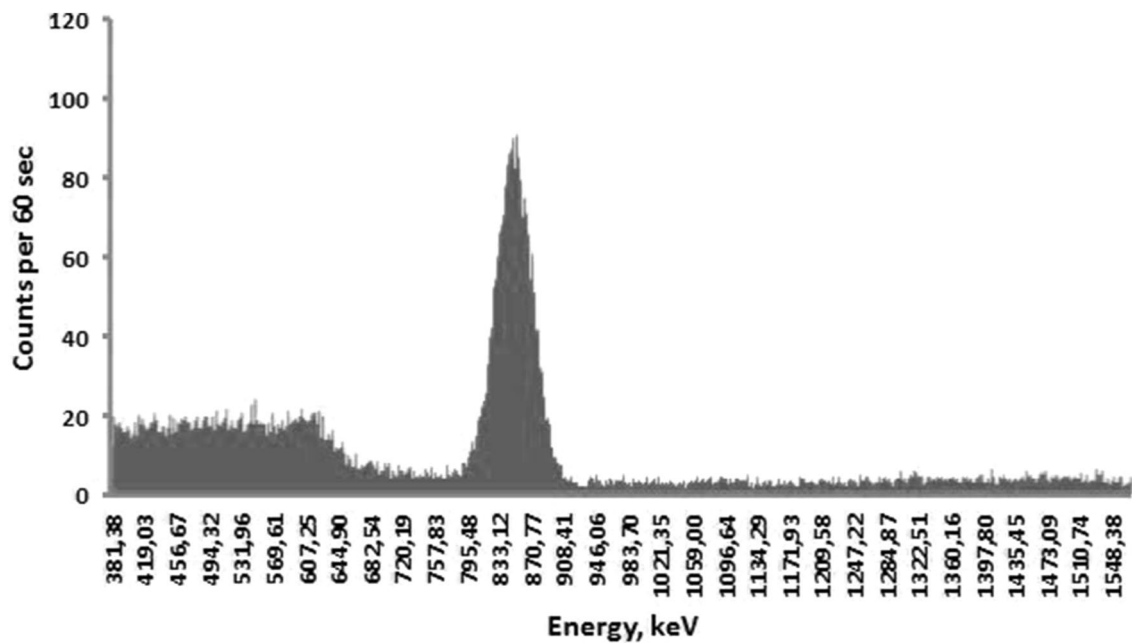
Fig. 3 Gamma spectrum of ^{56}Mn obtained from the sample of the lung of a mouse. The maximal peak corresponds to the 846.8 keV gamma energy (intensity—98.9%) of ^{56}Mn. Background gamma spectrum measured in the shielded room was subtracted
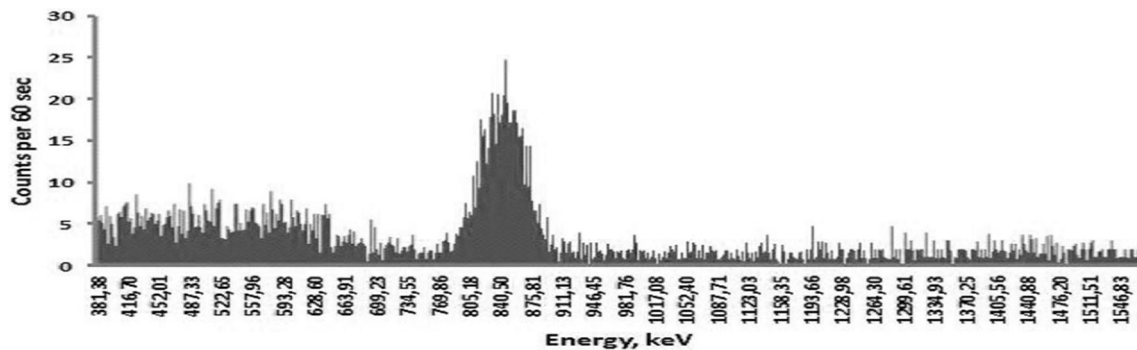

Fig. 4 Gamma spectrum of ^{56}Mn obtained from the sample of the lung of a rat. The maximal peak corresponds to the 846.8 keV gamma energy (intensity—98.9%) of ^{56}Mn. Background gamma spectrum measured in the shielded room was subtracted

rats (Stepanenko et al. 2017). A typical gamma spectra of ^{56}Mn measured by a gamma-spectrometer are presented in Figs. 3 and 4. In both examples with measured gamma spectrum of ^{56}Mn in biological samples, the amount of ^{56}MnO$_2$ powder dispersed over the experimental animals was equal. The background gamma spectrum measured in

a well-shielded room inside the reactor building is presented in Fig. 5.

Examples of calculated specific absorbed fractions (SAF—absorbed fraction of emitted energy per unit of organ's mass) for gammas and electrons as a function of energy are shown in Figs. 6, 7, 8, 9.
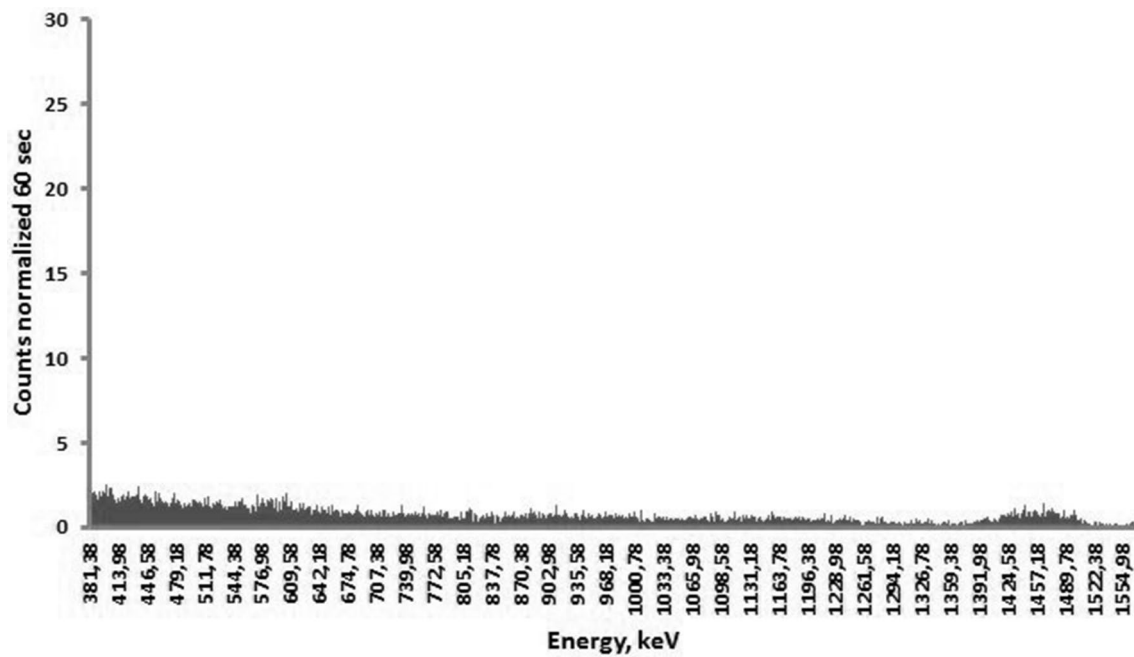
Fig. 5 Background gamma spectrum measured in a well-shielded "measuring lab" without any radioactive samples
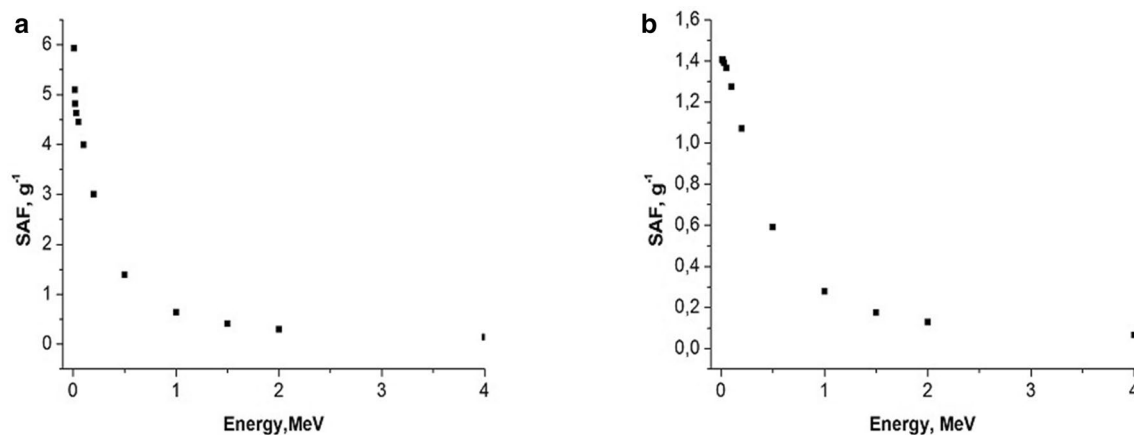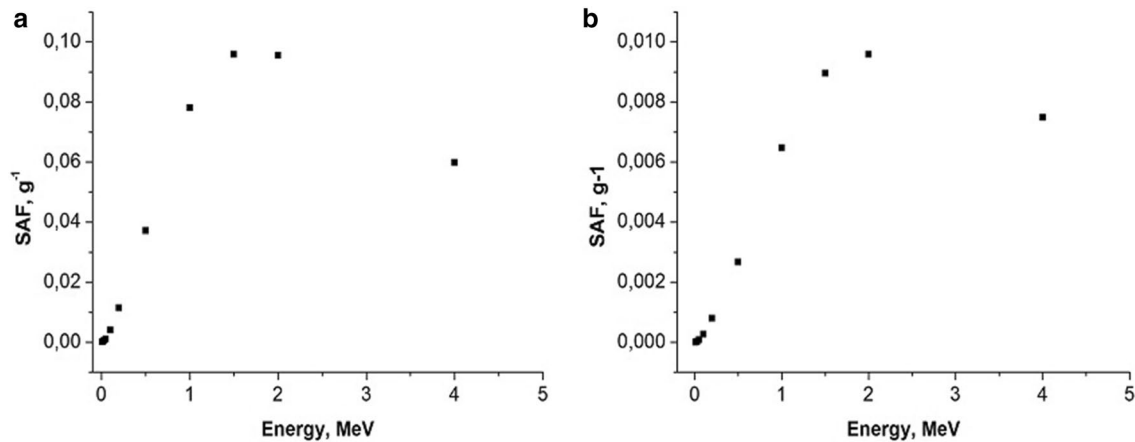

Fig. 6 Self-irradiation of lungs by electrons as a function of energy, MeV. Left panel: mouse, right panel: rat. Whole body weight of mouse (**a**): 30 g; whole body weight of rat (**b**): 270 g. SAF, g^{-1}: specific absorbed fraction of electron energy

Accumulated doses of internal irradiation were estimated from the beginning of exposure until infinity. It was assumed that physical decay of ^{56}Mn was essentially faster than biological redistribution of MnO$_2$ powder in the experimental animals. Results of internal dose estimations are presented in Tables 2 and 3.
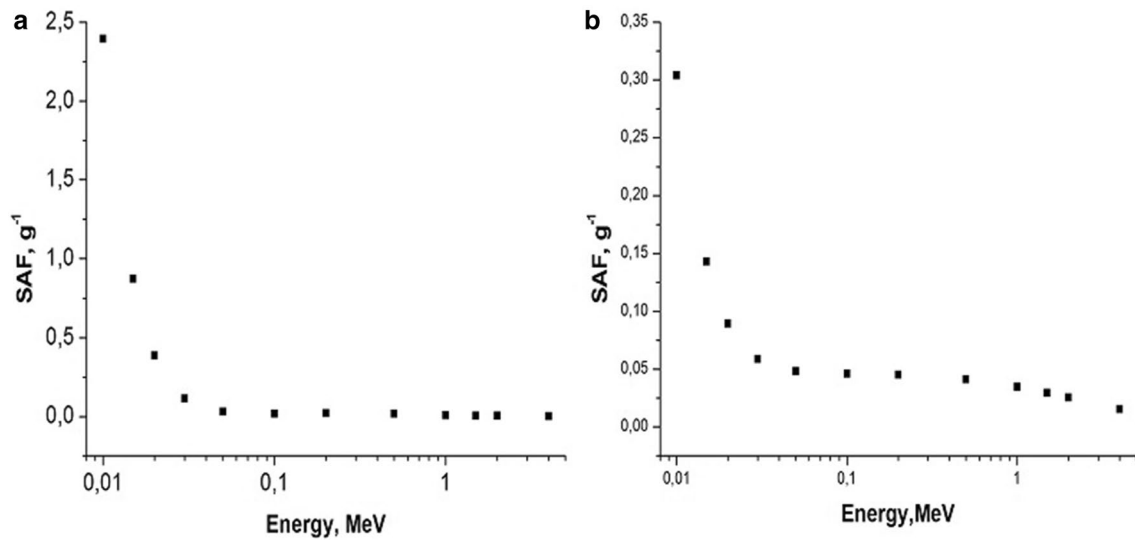
Fig. 7 Self-irradiation of lungs by gammas as a function of energy, MeV. Left panel: mouse, right panel: rat. Whole body weight of mouse (**a**): 30 g; whole body weight of rat (**b**): 270 g; SAF, g^{-1}: specific absorbed fraction of gamma energy

Fig. 8 Small intestine irradiating large intestine with electrons as a function of energy, MeV. Left panel: mouse; right panel: rat. Whole body weight of a mouse (**a**): 30 g; whole body weight of a rat (**b**): 270 g; SAF, g^{-1}: specific absorbed fraction of electron energy
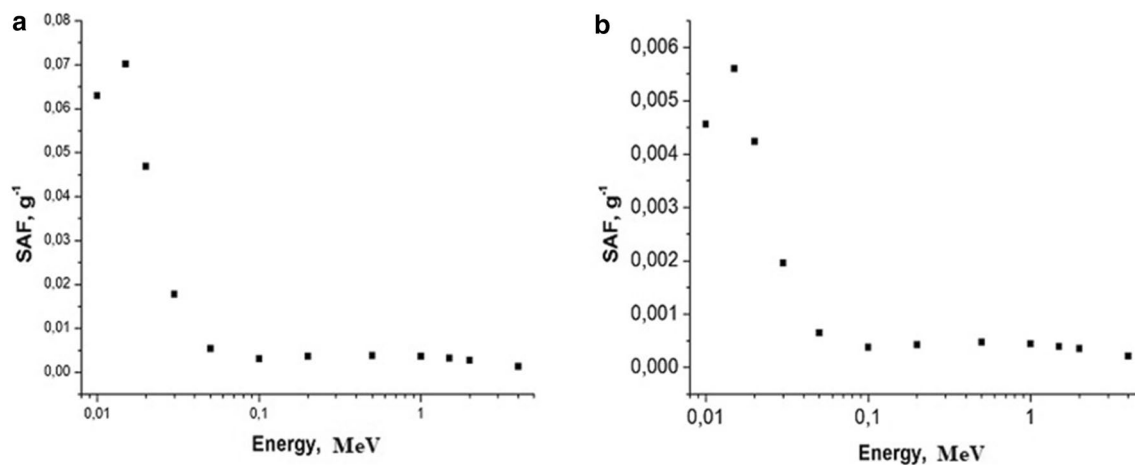
Fig. 9 Small intestine irradiating large intestine with gammas as function of energy, MeV. Left panel: mouse, right panel: rat. Whole body weight of a mouse (**a**): 30 g; whole body weight of a rat (**b**): 270 g; SAF, g^{-1}: specific absorbed fraction of gamma energy

Table 2 Doses of internal irradiation and corresponding standard deviations ($D \pm$ SD, Gy) in organs of experimental rats resulted from exposure to various activity levels of neutron-activated $^{56}MnO_2$ powder

Organs of Wistar rats	Initial activity of 100 mg dispersed $^{56}MnO_2$: 2.74×10^8 Bq $D \pm$ SD, Gy	Initial activity of 100 mg dispersed $^{56}MnO_2$: 5.5×10^8 Bq $D \pm$ SD, Gy	Initial activity of 100 mg dispersed $^{56}MnO_2$: 8.0×10^8 Bq $D \pm$ SD, Gy
Lungs	0.025 ± 0.004	0.048 ± 0.011	0.065 ± 0.013
Heart	0.0011 ± 0.0002	0.0039 ± 0.0012	0.0083 ± 0.0012
Small intestine	0.17 ± 0.02	0.42 ± 0.07	0.61 ± 0.14
Large intestine	0.29 ± 0.06	0.52 ± 0.11	0.76 ± 0.17
Stomach	0.09 ± 0.01	0.21 ± 0.02	0.30 ± 0.05
Esophagus	0.0069 ± 0.0012	0.016 ± 0.002	0.025 ± 0.006
Liver	0.0015 ± 0.0003	0.0045 ± 0.0012	0.0071 ± 0.0016
Spleen	0.00028 ± 0.00007	0.00050 ± 0.00011	0.00083 ± 0.00019
Kidney	0.00027 ± 0.00006	0.00064 ± 0.00012	0.00098 ± 0.00018
Trachea	0.0058 ± 0.0011	0.0120 ± 0.0024	0.019 ± 0.004
Skin	0.071 ± 0.021	0.110 ± 0.023	0.142 ± 0.028
Eyes	0.019 ± 0.004	0.041 ± 0.008	0.062 ± 0.012

Numbers of rats in each cage for each irradiation were different, that is, from 6 to 9 (rats) per cage

Table 3 Doses of internal irradiation and corresponding standard deviations ($D \pm$ SD, Gy) in organs of experimental mice resulted from exposure to various activity levels of neutron-activated $^{56}MnO_2$ powder

Organs of mice	Initial activity of 100 mg dispersed $^{56}MnO_2$: 8×10^7 Bq $D \pm$ SD, Gy, (C57Bl mice)	Initial activity of 100 mg dispersed $^{56}MnO_2$: 2.74×10^8 Bq $D \pm$ SD, Gy, (C57Bl mice)	Initial activity of 100 mg dispersed $^{56}MnO_2$: 2.74×10^8 Bq $D \pm$ SD, Gy, (C57Bl mice)	Initial activity of 100 mg dispersed $^{56}MnO_2$: 2.74×10^8 Bq $D \pm$ SD, Gy, (BALB/C mice)	Initial activity of 100 mg dispersed $^{56}MnO_2$: 2.74×10^8 Bq $D \pm$ SD, Gy, (CD-1 mice)	Initial activity of 100 mg dispersed $^6MnO_2$: 8×10^8 Bq $D \pm$ SD, Gy, (C57Bl mice)	Initial activity of 100 mg dispersed $^{56}MnO_2$: 8×10^8 Bq $D \pm$ SD, Gy, (C57Bl mice)	Initial activity of 100 mg dispersed $^{56}MnO_2$: 8×10^8 Bq $D \pm$ SD, Gy, (BALB/C mice)
Lungs	0.026 ± 0.005	0.096 ± 0.013	0.14 ± 0.02	0.11 ± 0.03	0.12 ± 0.02	0.25 ± 0.05	0.34 ± 0.07	0.38 ± 0.07
Heart	0.021 ± 0.005	0.056 ± 0.011	0.07 ± 0.01	0.061 ± 0.014	0.089 ± 0.017	0.12 ± 0.02	0.18 ± 0.04	0.15 ± 0.04
Small intestine	0.25 ± 0.09	0.91 ± 0.15	1.1 ± 0.2	0.86 ± 0.21	1.4 ± 0.3	2.3 ± 0.2	2.8 ± 0.4	2.4 ± 0.4
Large intestine	1.2 ± 0.16	4.2 ± 0.5	4.5 ± 0.5	3.8 ± 0.6	3.4 ± 0.5	10.1 ± 1.4	11 ± 2.1	9.5 ± 2.1
Stomach	0.27 ± 0.08	0.98 ± 0.16	1.2 ± 0.2	0.91 ± 0.22	0.81 ± 0.12	2.4 ± 0.5	2.2 ± 0.3	3.2 ± 0.5
Esophagus	0.032 ± 0.005	0.087 ± 0.013	0.079 ± 0.013	0.093 ± 0.016	0.052 ± 0.011	0.29 ± 0.05	0.17 ± 0.024	0.21 ± 0.04
Liver	0.0018 ± 0.0007	0.0066 ± 0.0011	0.0086 ± 0.0014	0.0076 ± 0.0012	0.0081 ± 0.0016	0.023 ± 0.002	0.022 ± 0.004	0.024 ± 0.005
Spleen	0.0006 ± 0.0001	0.0025 ± 0.0007	0.0028 ± 0.0006	0.0032 ± 0.0008	0.0036 ± 0.0007	0.006 ± 0.001	0.008 ± 0.002	0.007 ± 0.002
Kidney	0.0007 ± 0.0001	0.0028 ± 0.0005	0.0021 ± 0.0006	0.0026 ± 0.0004	0.0023 ± 0.0006	0.007 ± 0.002	0.006 ± 0.002	0.007 ± 0.002
Trachea	0.015 ± 0.004	0.039 ± 0.003	0.047 ± 0.008	0.05 ± 0.01	0.041 ± 0.009	0.14 ± 0.06	0.16 ± 0.04	0.13 ± 0.03
Skin	0.12 ± 0.03	0.29 ± 0.05	0.34 ± 0.06	0.31 ± 0.07	0.42 ± 0.09	0.96 ± 0.21	0.91 ± 0.16	0.99 ± 0.23
Eyes	0.041 ± 0.009	0.14 ± 0.05	0.13 ± 0.02	0.16 ± 0.03	0.12 ± 0.03	0.39 ± 0.08	0.32 ± 0.07	0.34 ± 0.07

Numbers of mice in each cage for each irradiation were different, that is, from 3 to 10 animals per cage

Discussion

In the present study, we found that under similar exposure conditions to $^{56}MnO_2$ powder, the internal doses in mice were several times higher in comparison with rats. This can, perhaps, be explained by the following: higher breathing rate in mice versus rats and, lower organ weight in mice compared with rats (Besyadovsky et al. 1978). It should be noted that the latter circumstance leads to the fact that the specific absorbed fraction of energy (that is, fraction of absorbed energy per unit mass of the organ) is essentially higher in mice than in rats (see Figs. 6, 7, 8, 9). Difference in doses of internal irradiation

of mice with the same activity of $^{56}MnO_2$ powder dispersed over the experimental animals can be explained by the fact that the number of mice per cage was different during different irradiation sessions (see Table 3 with corresponding note). This can also explain the absence of a simple proportionality between the internal radiation doses and the dispersed activity of $^{56}MnO_2$ (Tables 2 and 3). The increased doses in the lungs are explained by the fact that this organ is critical when inhaling small radioactive particles of $^{56}MnO_2$, which leads to an increased accumulation of activity in this organ. High doses of irradiation of the gastrointestinal tract can be explained by the fact that in the process of cleaning and grooming, experimental animals swallowed radioactive particles retained by their hair, which led to a high accumulation of activity in the stomach and intestines during exposure (1 h), as it was noted in Stepanenko et al. (2017), Shichijo et al. (2017). The retention of radioactive particles by animal hair leads to an increase in skin radiation dose.

Conclusion

This study aimed to estimate internal doses in laboratory animals (mice and rats) that had been exposed to various levels of $^{56}MnO_2$ in the form of dispersed powder. The experiment was performed in support of the Japanese initiative to investigate the biological effects of irradiation from residual neutron-activated radioactivity that resulted from the A-bombing (Hoshi 2020; Roesch 1987; Imanaka et al. 2012; Kerr et al. 2013, 2015; Ohtaki et al. 2014). Radionuclide ^{56}Mn ($T_{1/2} = 2.58$ h) is one of the main neutron-activated emitters during the first hours after neutron activation of soil dust particles.

In our previous studies (Stepanenko et al. 2017; Shichijo et al. 2017) related to irradiation of male Wistar rats after dispersion of $^{56}MnO_2$ powder, the internal doses in rats were found to be very inhomogeneous: distribution of doses among different organs ranged from 1.3 Gy in small intestine to less than 0.0015 Gy in some of the other organs. Internal doses in the lungs ranged from 0.03 to 0.1 Gy. The essential pathological changes were found in lung tissue of rats despite a low level of irradiation.

In the present study, the dosimetry investigations were extended: internal doses in experimental mice and rats were estimated for various activity levels of dispersed neutron-activated $^{56}MnO_2$ powder.

The following findings were noted:

(a) Internal radiation doses in mice were several times higher in comparison with rats under similar conditions of exposure to $^{56}MnO_2$ powder.

(b) When 2.74×10^8 Bq of $^{56}MnO_2$ powder was dispersed over mice, doses of internal irradiation ranged from 0.81

to 4.5 Gy in the gastrointestinal tract (small intestine, stomach, large intestine), from 0.096 to 0.14 Gy in lungs, and doses in skin and eyes ranged from 0.29 to 0.42 Gy and from 0.12 to 0.16 Gy, respectively. Internal radiation doses in other organs of mice were much lower.

(c) Internal radiation doses were significantly lower in organs of rats with the same activity of exposure to $^{56}MnO_2$ powder (2.74×10^8 Bq): 0.09, 0.17, 0.29, and 0.025 Gy in stomach, small intestine, large intestine, and lungs, respectively.

(d) Doses of internal irradiation in organs of rats and mice were two to four times higher when they were exposed to 8.0×10^8 Bq of $^{56}MnO_2$ (in comparison with exposure to 2.74×10^8 Bq of $^{56}MnO_2$).

(e) Internal radiation doses in organs of mice were 7–14 times lower with the lowest $^{56}MnO_2$ amount (8.0×10^7 Bq) in comparison with the highest amount, 8.0×10^8 Bq, of dispersed $^{56}MnO_2$ powder.

The data obtained will be used for interpretation of biological effects in experimental mice and rats that result from dispersion of various levels of neutron-activated $^{56}MnO_2$ powder, which is the subject of separate studies.

Compliance with ethical standards

Conflicts of interest The authors of this paper have no conflicts of interest according to their disclosure forms.

References

Be M-M, Chiste V, Dulieu C, Mougeot X, Browne E, Baglin C, Chechnev VP, Egorov A, Kuzmenko NK, Sergeev VO, Kondev FG, Luca A, Galan M, Huang X, Wang B, Helmer RG, Schonfeld E,

Dersch R, Vanin VR, de Castro RM, Nichols AL, MacMahon TD, Pearce A, Arinc A, Lee KB, Wu SC (2013) Table of radionuclides (Comments on evaluation). Volumes 1–7, Bureau International des Poids et Mesures. Paviollon de Breteuil, F-92310 SEVRES. https://www.bipm.org/utils/common/pdf/monographieRI/Monographie_BIPM-5_Tables_Vol7.pdf .Accessed 20 Feb 2020

Besyadovsky RA, Ivanov KV, Kozyura AK (1978) Handbook for the radiobiologists. Moscow. Atomizdat. pp. 78 (in Russian). https://www.ozon.ru/context/detail/id/17918088/. Accessed 20 Feb 2020

Bolch WE, Eckerman KF, Sgouros G, Thomas R (2009) MIRD Pamphlet No. 21: a generalized schema for radiopharmaceutical dosimetry-standardization of nomenclature. J Nucl Med 50(3):477–484. https://doi.org/10.2967/jnumed.108.056036. http://www.hopkinsmedicine.org/RTD_lab/pdf/2009_JNM_MIRD_P21_schema.pdf. Accessed 20 Feb 2020

Briemeister JF (2000) MCNP–A general Monte–Carlo N–particle transport code. In: Version 4C. Los Alamos. Los Alamos National Laboratory, USA

Directive 2010/63/EU of the European Parliament and the Council of the Office on the protection of animals used for scientific purposes of 22 September 2010 (2010) Official Journal of the European Union. L 276: 33–79. https://eur-lex.europa.eu/LexUriServ/LexUriServ.do?uri=OJ:L:2010:276:0033:0079:EN:PDF. Accessed 20 February 2020

Hoshi M (2020) A long history exploring radiation exposure. Impact, pp 70–72. https://www.ingentaconnect.com/content/sil/impact/2020/00002020/00000003/art00026?crawler=true&mimetype=application/pdf

Imanaka T, Endo S, Kawano N, Tanaka K (2012) Radiation exposure and disease questionnaires of early entrants after the Hiroshima bombing. Radiat Protect Dosim 149(1): 91–96. https://doi.org/10.1093/rpd/ncr370. https://www.ncbi.nlm.nih.gov/pubmed/21914640. Accessed 20 Feb 2020

Kerr GD, Egbert SD, Al-Nabulsi I, Beck HL, Cullings HM, Endo S, Hoshi M, Imanaka T, Kaul DC, Maruyama S, Reeves GI, Ruehm W, Sakaguchi A, Simon SL, Spriggs GD, Stram DO, Tonda T, Weiss JF, Weitz RL, Young RW (2013) Workshop report on atomic bomb dosimetry—residual radiation exposure: recent research and suggestions for future studies. Health Phys 105(2):140–149. https://doi.org/10.1097/hp.0b013e31828ca73a. http://energy.gov/ehss/downloads/workshop-report-health-physics-journal. Accessed 20 Feb 2020

Kerr GD, Egbert SD, Al-Nabulsi I, Bailiff IK, Beck HL, Belukha IG, Cockayne JE, Cullings HM, Eckerman KF, Granovskaya E, Grant EJ, Hoshi M, Kaul DC, Kryuchkov V, Mannis D, Ohtaki M, Otani K, Shinkarev S, Simon SL, Spriggs GD, Stepanenko VF, Stricklin D, Weiss JF, Weitz RL, Woda C, Worthington PR, Yamamoto K, Young RW (2015) Workshop report on atomic bomb dosimetry—a review of dose related factors for the evaluation of exposures to residual radiation at Hiroshima and Nagasaki. Health Phys 109(6):582–600. https://doi.org/10.1097/hp.0000000000000395. https://www.ncbi.nlm.nih.gov/pubmed/26509626. Accessed 20 Feb 2020

Lanin A (2013) Nuclear rocket engine reactor. Springer Ser Mater Sci 170:1. Springer, Berlin, Heidelberg. https://doi.org/10.1007/978-3-642-32430-7_1. https://www.springer.com/gp/book/9783642324291. Accessed 20 Feb 2020

Ohtaki M, Otani K, Tonda T, Sato Y, Hara N, Imori S, Matsui C, Kawakami H, Tashiro S, Aihara K, Hoshi M, Satoh K (2014) Effect of distance from hypocenter at exposure on solid cancer mortality among Hiroshima atomic bomb survivors with very low initial radiation dose in the Dosimetry System 1986 (DS86). Health Phys 107(1):S45

Roesch WC (eds) (1987) US—Japan Joint Reassessment of Atomic Bomb Radiation Dosimetry in Hiroshima and Nagasaki, Final Report-Dosimetry System 1986 (DS86). Radiation Effects Research Foundation. Hiroshima. http://www.rerf.jp/library/index_e.html. Accessed 20 Feb 2020

Shichijo K, Fujimoto N, Uzbekov D, Kairkhanova Y, Saimova A, Chaizhunusova N, Sayakenov N, Shabdarbaeva D, Aukenov N, Azimkhanov A, Kolbayenkov A, Mussazhanova Z, Niino D, Nakashima M, Zhumadilov K, Stepanenko V, Tomonaga M, Rakhypbekov T, Hoshi M (2017) Internal exposure to neutron-activated ^{56}Mn dioxide powder in Wistar rats—part 2: pathological effects. Radiat Environ Biophys 56(1):55–61. https://doi.org/10.1007/s00411-016-0676-z. https://link.springer.com/article/10.1007/s00411-016-0676-z. Accessed February 20, 2020

Stabin M, Hunt SJ, Sparks R, Lipsztein J, Eckerman J (2001) RADAR: the radiation dose assessment resource–an online source of dose information for nuclear medicine and occupation radiation safety. J Nucl Med 42:243

Stepanenko VF, Iaskova EK, Belukha IG, Petriev VM, Skvortsov VG, Kolyzhenkov TV, Petukhov AD, Dubov DV (2015) The calculation of internal irradiation of nano-, micro- and macro-biostructures by electrons, beta particles and quanta radiation of different energy for the development and research of new radiopharmaceuticals in nuclear medicine. Radiation and risk. Bull Natl Radiat Epidemiol Registry 24(1):35–60

Stepanenko V, Rakhypbekov T, Otani K, Endo S, Satoh K, Kawano N, Shichijo K, Nakashima M, Takatsuji T, Sakaguchi A, Kato H, Onda Y, Fujimoto N, Toyoda S, Sato H, Dyussupov A, Chaizhunusova N, Sayakenov N, Uzbekov D, Saimova A, Shabdarbaeva D, Skakov M, Vurim A, Gnyrya V, Azimkhanov A, Kolbayenkov A, Zhumadilov K, Kairikhanova Y, Kaprin A, Galkin V, Ivanov S, Kolyzhenkov T, Petukhov A, Yaskova E, Belukha I, Khailov A, Skvortsov V, Ivannikov A, Akhmedova U, Bogacheva V, Hoshi M (2017) Internal exposure to neutron-activated ^{56}Mn dioxide powder in Wistar rats—part 1: dosimetry. Radiat Environ Biophys 56: 47–54. https://doi.org/10.1007/s00411-016-0678-x. https://www.ncbi.nlm.nih.gov/pubmed/28188481. Accessed 20 Feb 2020

Tanaka K, Endo S, Imanaka T, Shizuma K, Hasai H, Hoshi M (2008) Skin dose from neutron-activated soil for early entrants following the A-bomb detonation in Hiroshima: contribution from beta and gamma rays. Radiat Environ Biophys 47:323–330. https://doi.org/10.1007/s00411-008-0172-1. https://www.ncbi.nlm.nih.gov/pubmed/18496704. Accessed 20 Feb 2020

Weitz R (2014) Reconstruction of beta-particle and gamma-ray doses from neutron activated soil at Hiroshima and Nagasaki. Health Phys 107(1):S43

Affiliations

Valeriy Stepanenko[1] · Andrey Kaprin[2] · Sergey Ivanov[1] · Peter Shegay[2] · Kassym Zhumadilov[3] ·
Aleksey Petukhov[1] · Timofey Kolyzhenkov[1] · Viktoria Bogacheva[1] · Elena Zharova[2] · Elena Iaskova[1] ·
Nailya Chaizhunusova[4] · Dariya Shabdarbayeva[4] · Gaukhar Amantayeva[4] · Arailym Baurzhan[4] · Bakhyt Ruslanova[4] ·
Zhaslan Abishev[4] · Madina Apbassova[4] · Ynkar Kairkhanova[4] · Darkhan Uzbekov[4] · Zaituna Khismetova[4] ·
Yersin Zhunussov[4] · Nariaki Fujimoto[5] · Hitoshi Sato[6] · Kazuko Shichijo[7] · Masahiro Nakashima[7] · Aya Sakaguchi[8] ·
Shin Toyoda[9] · Noriyuki Kawano[10] · Megu Ohtaki[5] · Keiko Otani[10] · Satoru Endo[11] · Masayoshi Yamamoto[12] ·
Masaharu Hoshi[10]

[1] Medical Radiological Research Center named after A.F. Tsyb-branch of "National Medical Research Center of Radiology" Ministry of Health of the Russian Federation, Koroleva Str. 4, Obninsk 249036, Kaluga, Russian Federation

[2] National Medical Research Center of Radiology, Ministry of Health of the Russian Federation, Koroleva Str. 4, Obninsk 249036, Kaluga, Russian Federation

[3] Eurasian National University named after L.N. Gumilyov, Astana, 2 Satpayev Str., Nur-Sultan 010000, Republic of Kazakhstan

[4] Semey Medical University, 103 Abay Str., Semey 071400, Republic of Kazakhstan

[5] Research Institute for Radiation Biology and Medicine, Hiroshima University, 1-2-3, Kasumi, Minami-ku, Hiroshima 734-8551, Japan

[6] Ibaraki Prefectural University of Health Sciences, 4669-2 Ami-chyo Ami, Inashiki-gun, Ibaraki 300-0394, Japan

[7] Atomic Bomb Disease, Institute, Nagasaki University, 1-12-4, Sakamoto, Nagasaki 852-8102, Japan

[8] Faculty of Pure and Applied Sciences, University of Tsukuba, 1-1-1, Tsukuba-shi Tennodai, Ibaraki 305-8571, Japan

[9] Department of Applied Physics, Okayama University of Science, 1-1 Ridai, Kita-ku, Okayama 700-0005, Japan

[10] The Center for Peace, Hiroshima University, Higashisenda-machi 1-1-89, Naka-ku, Hiroshima 730-0053, Japan

[11] Graduate School of Engineering, Hiroshima University, 1-4-1, Kagamiyama, Higashi, Hiroshima 739-8527, Japan

[12] Graduate School of Natural Science and Technology, Kanazawa University, Kakuma-Cho, Kanazawa 920-1192, Japan